JOURNAL OF THE AMERICAN COLLEGE OF CARDIOLOGY
© 2014 BY THE AMERICAN COLLEGE OF CARDIOLOGY FOUNDATION
PUBLISHED BY ELSEVIER INC.

VOL. 64, NO. 14, 2014
ISSN 0735-1097/$36.00
http://dx.doi.org/10.1016/j.jacc.2014.05.069

Quantitative Assessment of Myocardial Perfusion in the Detection of Significant Coronary Artery Disease

Cutoff Values and Diagnostic Accuracy of Quantitative [^{15}O]H_2O PET Imaging

Ibrahim Danad, MD,* Valtteri Uusitalo, MD,† Tanja Kero, MD,‡ Antti Saraste, MD, PhD,† Pieter G. Raijmakers, MD, PhD,§ Adriaan A. Lammertsma, PhD,§ Martijn W. Heymans, PhD,‖ Sami A. Kajander, MD, PhD,† Mikko Pietilä, MD, PhD,† Stefan James, MD, PhD,¶ Jens Sörensen, MD, PhD,‡ Paul Knaapen, MD, PhD,* Juhani Knuuti, MD, PhD†

ABSTRACT

BACKGROUND Recent studies have demonstrated improved diagnostic accuracy for detecting coronary artery disease (CAD) when myocardial blood flow (MBF) is quantified in absolute terms, but there are no uniformly accepted cutoff values for hemodynamically significant CAD.

OBJECTIVES The goal of this study was to determine cutoff values for absolute MBF and to evaluate the diagnostic accuracy of quantitative [^{15}O]H_2O positron emission tomography (PET).

METHODS A total of 330 patients underwent both quantitative [^{15}O]H_2O PET imaging and invasive coronary angiography in conjunction with fractional flow reserve measurements. A stenosis >90% and/or fractional flow reserve ≤0.80 was considered obstructive; a stenosis <30% and/or fractional flow reserve >0.80 was nonobstructive.

RESULTS Hemodynamically significant CAD was diagnosed in 116 (41%) of 281 patients who fulfilled study criteria for CAD. Resting perfusion was 1.00 ± 0.25 and 0.92 ± 0.23 ml/min/g in regions supplied by nonstenotic and significantly stenosed vessels, respectively ($p < 0.001$). During stress, perfusion increased to 3.26 ± 1.04 ml/min/g and 1.73 ± 0.67 ml/min/g, respectively ($p < 0.001$). The optimal cutoff values were 2.3 and 2.5 for hyperemic MBF and myocardial flow reserve, respectively. For MBF, these cutoff values showed a sensitivity, specificity, and accuracy for detecting significant CAD of 89%, 84%, and 86%, respectively, at a per-patient level and 87%, 85%, and 85% at a per-vessel level. The corresponding myocardial flow reserve values were 86%, 72%, and 78% (per patient) and 80%, 82%, and 81% (per vessel). Age and sex significantly affected diagnostic accuracy of quantitative PET.

CONCLUSIONS Quantitative MBF measurements with the use of [^{15}O]H_2O PET provided high diagnostic performance, but both sex and age should be taken into account. (J Am Coll Cardiol 2014;64:1464–75) © 2014 by the American College of Cardiology Foundation.

From the *Department of Cardiology, VU University Medical Center, Amsterdam, the Netherlands; †Turku University Hospital and University of Turku, Turku, Finland; ‡Department of Nuclear Medicine and PET, Institution of Radiology, Oncology and Radiation Science, Institute of Medical Sciences, Uppsala University, Uppsala, Sweden; §Department of Nuclear Medicine & PET Research, VU University Medical Center, Amsterdam, the Netherlands; ‖Department of Epidemiology and Biostatistics, VU University Medical Center, Amsterdam, the Netherlands; and the ¶Department of Cardiology, Institute of Medical Sciences, Uppsala University, Uppsala, Sweden. Dr. Lammertsma has received research grants from AVID, Philips Healthcare, F. Hoffmann-La Roche Ltd., and the European Commission. Dr. Knuuti is supported by the Academy of Finland Centre of Excellence in Molecular Imaging in Cardiovascular and Metabolic Research, Helsinki, Finland; has received grant support from Gilead Inc.; and is a consultant to Lantheus Inc. All other authors have reported that they have no relationships relevant to the contents of this paper to disclose.

Listen to this manuscript's audio summary by *JACC* Editor-in-Chief Dr. Valentin Fuster.
You can also listen to this issue's audio summary by *JACC* Editor-in-Chief Dr. Valentin Fuster.

Manuscript received February 3, 2014; revised manuscript received May 2, 2014, accepted May 13, 2014.

Increasingly, cardiac positron emission tomography (PET) is being used to noninvasively assess myocardial blood flow (MBF). Traditionally, nuclear myocardial perfusion imaging (MPI) is based on the interpretation of static tracer uptake images. However, in contrast to single-photon emission computed tomography MPI, PET can quantify MBF in absolute terms (1-4). Current commercially available PET technology has paved the way for routine quantification of MBF.

SEE PAGE 1476

Several PET tracers, such as rubidium-82 (^{82}Rb), ^{13}N-ammonia ($^{13}NH_3$), and [^{15}O]H_2O, have been well validated and routinely used in clinical practice (5-7). Recent studies have demonstrated the incremental diagnostic value of quantitative MBF measurements above visual grading of tracer uptake images (8,9). One of the fundamental issues when interpreting quantitative hyperemic MBF results is to define optimal cutoff values for distinguishing between normal and pathological MBF in hemodynamically compromised epicardial disease. Although previous studies have reported discriminatory values of hyperemic MBF and myocardial flow reserve (MFR) (10-17), these studies were hampered by the lack of a gold standard identifying flow-limiting coronary stenosis and limitations inherent in single-center studies.

The worldwide interest in quantitative cardiac PET necessitates use of uniform thresholds to facilitate patient management, exchange of patient data, and large multicenter studies that will enforce tighter guidelines. Although studies have evaluated diagnostic performance of qualitative cardiac PET imaging (9,12,15,17), few data exist on the diagnostic accuracy of quantitative cardiac PET imaging. Therefore, the goal of the present study was to determine optimal diagnostic cutoff values of myocardial perfusion as assessed with quantitative [^{15}O]H_2O PET in a clinical cohort of patients with suspected coronary artery disease (CAD). Patients in a large collaborative PET study underwent both PET MPI and invasive coronary angiography (ICA) in conjunction with fractional flow reserve (FFR) assessment. The diagnostic accuracy of absolute hyperemic MBF and MFR to detect hemodynamically significant CAD as indicated by FFR was assessed, as was the impact of sex, age, and CAD risk profile on absolute MBF.

METHODS

STUDY POPULATION. Three institutions participated in this collaborative PET study: VU University Medical Center (n = 163), Turku University Hospital (n = 161), and Uppsala University Hospital (n = 6). The study flow chart is depicted in Figure 1. With symptoms suggestive of CAD, patients had been referred for ICA and then prospectively enrolled to undergo [^{15}O]H_2O PET before ICA. A total of 330 patients were included. No cardiac events were documented between PET studies and ICA. Exclusion criteria were atrial fibrillation, second- or third-degree atrioventricular block, symptomatic asthma, pregnancy, or a documented history of CAD, (defined as a previous percutaneous coronary intervention, coronary artery bypass graft surgery, or myocardial infarction). In all patients, electrocardiography showed no signs of a previous myocardial infarction, and echocardiography, when performed, showed normal left ventricular function without wall motion abnormalities. CAD pre-test likelihood was determined according to the Diamond and Forrester criteria (18) by using cutoffs of <13.4% and >87.2%, for low and high pre-test likelihoods, respectively, and intermediate pre-test likelihood for values between these 2 cutoffs. Each center had institutional review board approval for the study.

POSITRON EMISSION TOMOGRAPHY. Each patient underwent a [^{15}O]H_2O PET/computed tomography (CT) study by using a hybrid PET/CT scanner with

ABBREVIATIONS AND ACRONYMS

CAD = coronary artery disease
CI = confidence interval
CT = computed tomography
FFR = fractional flow reserve
ICA = invasive coronary angiography
MBF = myocardial blood flow
MFR = myocardial flow reserve
MPI = myocardial perfusion imaging
NPV = negative predictive value
PET = positron emission tomography
PPV = positive predictive value
ROC = receiver-operator characteristic

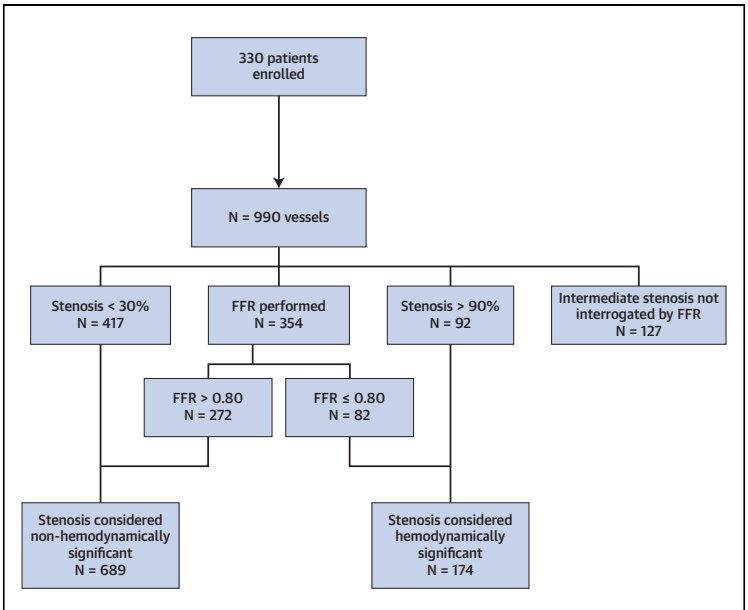

FIGURE 1 Study Flow Chart

Study flow chart showing the enrollment of patients and the number of coronary arteries interrogated by using fractional flow reserve (FFR).

site-specific protocols. Patients at the VU University Medical Center were scanned by using a Gemini TF 64 PET/CT scanner (Philips Healthcare, Best, the Netherlands). The PET scanning protocol has been described in detail previously (19). Patients at the Turku University Hospital were scanned on a Discovery VCT PET/CT scanner (GE Medical Systems, Waukesha, Wisconsin); this protocol was also previously described (15). Images were reconstructed by using GE's standard iterative reconstruction algorithm. The Uppsala University Hospital patients were scanned on a Discovery ST PET/CT scanner (GE Medical Systems) in 3-dimensional mode. A 6-min dynamic PET perfusion scan during resting conditions was started simultaneously with the administration of 400 MBq of $[^{15}O]H_2O$. After a 15-min delay following the first injection, an identical PET sequence was performed during hyperemia. To correct for photon attenuation and scatter, a single low-dose (10 mA) respiration-averaged CT scan during normal breathing was acquired just before the resting PET scan. Images were reconstructed by using the ordered subset expectation maximization algorithm (2 iterations, 28 subsets) into 22 frames (1×10, 8×5, 4×10, 2×15, 3×20, 2×30, and 2×60 s).

All institutions used adenosine to induce hyperemia, initiated 2 min before the stress scan for maximal vasodilation.

QUANTIFICATION OF MBF. Quantitative MBF images were generated by using 2 previously published software packages developed in-house: Cardiac VUer (used by VU University Medical Center and Uppsala University Hospital) and Carimas (Turku University Hospital) (11,20). Both packages extract the arterial input function directly from the dynamic PET data and use a single tissue compartment model with correction for perfusable tissue fraction to generate parametric MBF images (11,20,21). MBF was expressed in milliliters per minute per gram of perfusable tissue. To account for changes in baseline MBF caused by cardiac workload, baseline MBF values were corrected for rate-pressure product, an index of myocardial oxygen consumption, using the follow equation: corrected MBF = (MBF/rate-pressure product) $\times 10^4$ (22). Corrected MFR (MFR_{corr}) was defined as the ratio of hyperemic MBF divided by corrected baseline MBF.

ICA AND FFR. ICA imaging was performed according to standard clinical protocols. The coronary tree was divided into a 16-segment coronary artery model modified from the American Heart Association (23). All major coronary arteries and side branches >2.0 mm were interrogated with FFR. An FFR ≤0.80 was considered a hemodynamically significant stenosis, and an FFR >0.80 was nonsignificant. If FFR was missing, vessels with a <30% stenosis were considered functionally not relevant, whereas >90% coronary stenoses were graded as hemodynamically significant. The operators refrained from FFR measurement in tight lesions >90% to avoid potentially inflicting a coronary dissection with the pressure wire. All vessels containing an intermediate stenosis (30% to 90%) not interrogated with FFR were excluded from analysis. FFR was measured by using a 0.014-inch sensor-tipped guidewire, introduced through a 5- or 6-F guiding catheter. Furthermore, adenosine was infused using either intravenous (Turku University Hospital) or intracoronary (Uppsala University Hospital and VU University Medical Center) administration with a dosage of 140 μg/kg/min and 150 μg, respectively, in right and left coronary arteries to induce maximal coronary hyperemia. FFR was calculated as the ratio of mean distal intracoronary pressure, measured by pressure wire and mean arterial pressure measured with the coronary catheter (24).

INTERPRETATION OF PET IMAGING RESULTS. Data were analyzed on a per-patient and per-vessel basis. The 3 main vascular territories (right coronary artery,

TABLE 1 Characteristics of Study Population (N = 330)

Age, yrs	61 ± 9
Male	192 (58)
Length, m	1.72 ± 0.10
Weight, kg	80 ± 15
BMI, kg/m^2	27 ± 4
Coronary risk profile	
Diabetes mellitus type 2	45 (14)
Hypertension	153 (46)
Hypercholesterolemia	164 (50)
Smoking history	110 (33)
Family history of CAD	100 (30)
Medication	
Acetylsalicylic acid	269 (82)
Beta-blockers	208 (63)
Statins	230 (70)
ACE inhibitors	65 (20)
ARBs	51 (16)
CCBs	65 (20)
Type of chest pain	
Typical angina	115 (35)
Atypical angina	153 (46)
Aspecific chest pain	53 (16)
No chest discomfort/high-risk profile	9 (3)
Pre-test likelihood of CAD	
Low	20 (6)
Intermediate	270 (82)
High	40 (12)

Values are mean ± SD or n (%).

ACE = angiotensin-converting enzyme; ARBs = angiotensin II receptor blockers; BMI = body mass index; CAD = coronary artery disease; CCB = calcium channel blocker.

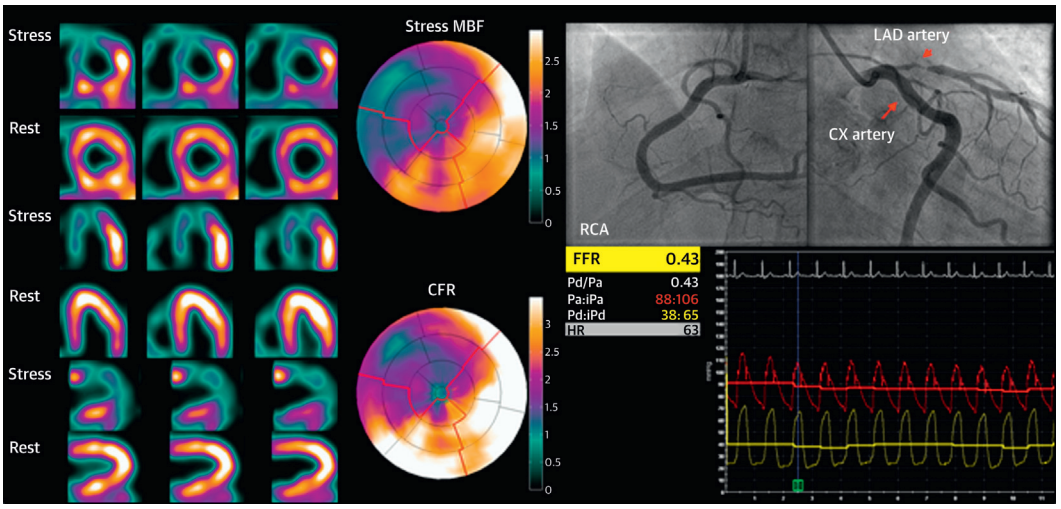

FIGURE 2 Male, 58-Year-Old Patient With Typical Anginal Chest Pain

Positron emission tomography (PET) showed a perfusion defect with an abnormal hyperemic perfusion of 1.26 ml/min/g and a myocardial flow reserve (MFR) of 1.61 in the area supplied by the left anterior descending (LAD) artery. Invasive coronary angiography showed angiographic significant >70% luminal narrowing of the LAD artery (1-vessel disease) with an FFR of 0.43. CX = circumflex artery; RCA = right coronary artery; other abbreviation as in Figure 1.

left anterior descending artery, and circumflex artery) were analyzed separately. Anatomical information obtained from ICA was used to assess coronary dominance and to allocate a coronary lesion to its subtended vascular territory on parametric MBF images based on the 17-myocardial segment model for all cardiac imaging of the American Heart Association (25). In addition, segmental analysis was performed, whereby a perfusion defect of at least 2 adjacent myocardial segments was assigned to the right coronary artery or circumflex artery vascular territory; a perfusion defect of at least 4 adjacent segments was assigned to the left anterior descending vascular territory. Subsequently, this regional perfusion value was used for further analyses instead of the mean of MBF or MFR of the predefined vascular territory to avoid impact of overlapping adjacent vascular regions.

STATISTICAL ANALYSIS. Continuous variables are presented as mean ± SD, whereas categorical variables are expressed as actual numbers. Continuous variables between FFR groups were compared by using the 2-sided Student *t* test. A receiver-operator characteristic (ROC) curve analysis and the Youden index were used to define PET perfusion cutoff values with the highest discriminative power. Comparison of ROC curves was performed by the method of deLong to calculate the SE of the area under the curve and the difference between ROC curves (26). Based on evidence from the literature (10,27), predictors associated with hyperemic MBF and MFR such as age, sex, and traditional cardiac risk factors were selected for univariate and multivariable linear regression analyses to examine their effect on myocardial

TABLE 2 Systemic Hemodynamics at Baseline and Hyperemia

	Total Study Population (N = 330)	Nonobstructive CAD (n = 165)	Obstructive CAD (n = 116)	p Value (Between-Group CAD)
Heart rate, beats/min				
Baseline	60 ± 9	61 ± 9	59 ± 9	0.16
Hyperemia	81 ± 14	83 ± 14	78 ± 12	0.01
p value	<0.001	<0.001	<0.001	
Systolic blood pressure, mm Hg				
Baseline	129 ± 24	125 ± 22	130 ± 26	0.10
Hyperemia	126 ± 23	122 ± 19	128 ± 27	0.06
p value	<0.001	0.14	0.03	
Diastolic blood pressure, mm Hg				
Baseline	67 ± 12	66 ± 11	67 ± 12	0.53
Hyperemia	65 ± 11	63 ± 10	65 ± 13	0.24
p value	<0.001	<0.01	0.02	
Mean arterial pressure, mm Hg				
Baseline	87 ± 14	85 ± 13	87 ± 15	0.21
Hyperemia	85 ± 14	82 ± 12	85 ± 16	0.15
p value	<0.001	0.06	0.04	
Rate-pressure product				
Baseline	7,805 ± 2,102	7,658 ± 2,068	7,720 ± 2,022	0.81
Hyperemia	10,284 ± 2,756	10,218 ± 2,580	9,948 ± 2,742	0.43
p value	<0.001	<0.001	<0.001	

Values are mean ± SD.
CAD = coronary artery disease.

perfusion. A linear mixed-effects model with per-patient random effects was used to account for the clustering of multiple vessel measurements. Diagnostic performance of quantitative PET for detecting flow-limiting CAD and angiographic obstructive epicardial disease was determined with sensitivity, specificity, negative predictive value (NPV), positive predictive value (PPV), and accuracy on a per-patient and per-vessel basis. Chi-square or McNemar tests were used, as appropriate, to compare diagnostic accuracy of quantitative PET with ICA in conjunction with FFR. A p value <0.05 was considered statistically significant. All statistical analyses were performed by using IBM SPSS Statistics version 20 (IBM SPSS Statistics, IBM Corporation, Armonk, New York) and MedCalc software 12.7.4.0 (MedCalc Software, Mariakerke, Belgium).

RESULTS

A total of 330 patients (Table 1) underwent both [^{15}O]H_2O PET and ICA in conjunction with FFR and were enrolled in the study (Figure 1). Obstructive CAD was diagnosed in 116 (41%) patients, with nonhemodynamically significant CAD observed in 165 (59%) patients who fulfilled study criteria for CAD. FFR values were obtained in 160 (48%) patients, of whom 30 (19%) received intravenous adenosine during FFR measurements, and 130 (81%) received intracoronary adenosine. FFR measurements were lacking in 49 (15%) patients with at least 1 intermediate coronary stenosis.

On a per-vessel analysis, 174 (17%) vessels contained a flow-limiting stenosis, while nonobstructive CAD was seen in 689 (70%) vessels (Figure 1). A total of 127 (13%) vessels were excluded from analysis because of a lack of FFR measurements to assess the hemodynamic relevance of an intermediate stenosis. Figure 2 illustrates a case in which angiographic significant CAD was proven to be hemodynamically significant according to both [^{15}O]H_2O PET and FFR measurements. Table 2 summarizes hemodynamic characteristics of all patients. Overall, during adenosine-induced hyperemia, heart rate and rate-pressure product increased significantly compared with baseline, whereas a decrease in both diastolic and systolic blood pressures was noted. When grouped according to FFR, there were no significant differences in hemodynamic parameters, except for heart rate during hyperemia, which was slightly lower in patients with functionally relevant CAD.

RELATIONSHIP BETWEEN FUNCTIONAL CAD SEVERITY AND MBF. On a per-patient level, global MBF was 0.99 ± 0.26 ml/min/g during resting conditions, increasing to 2.91 ± 1.09 ml/min/g during adenosine-induced hyperemia ($p < 0.001$), yielding an MFR of 3.05 ± 1.09. On a per-vessel basis, baseline flow increased from 0.98 ± 0.25 ml/min/g to 2.91 ± 1.14 ml/min/g during hyperemia ($p < 0.001$), yielding an MFR of 3.06 ± 1.19. Baseline and hyperemic MBF were significantly lower in areas subtended by vessels with hemodynamically significant stenoses compared with those without obstructive CAD: 0.92 ± 0.23 ml/min/g versus 1.00 ± 0.25 ml/min/g and 1.73 ± 0.67 ml/min/g versus 3.26 ± 1.04 ml/min/g (all $p < 0.001$) for baseline and hyperemic MBF, respectively (Figure 3). MFR and MFR_{corr} decreased significantly ($p < 0.001$), from

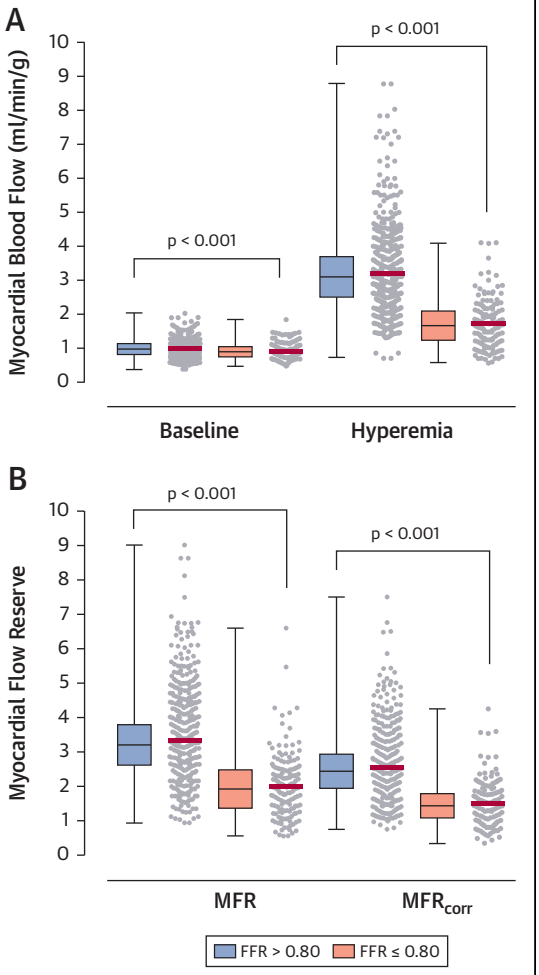

FIGURE 3 Quantitative Myocardial Perfusion in Relation to Functional Severity of CAD

(A) Baseline myocardial blood flow (MBF), hyperemic MBF, and **(B)** MFR in relation to functional coronary artery disease (CAD) severity as indicated by FFR. MFR_{corr} = myocardial flow reserve of which the baseline perfusion is corrected for the rate-pressure product; other abbreviations as in Figures 1 and 2.

3.37 ± 1.11 and 2.55 ± 0.93 to 1.99 ± 0.89 and 1.49 ± 0.63, respectively, in myocardial territories subtended by arteries with obstructive CAD.

DIAGNOSTIC PERFORMANCE OF QUANTITATIVE [^{15}O]H_2O PET FOR DETECTING FLOW-LIMITING DISEASE. Detecting hemodynamically significant CAD on a per-vessel basis produced area under the curve values for baseline MBF, hyperemic MBF, MFR, and MFR_{corr} of 0.60 (95% confidence interval [CI]: 0.55 to 0.64), 0.90 (95% CI: 0.88 to 0.93), 0.86 (95% CI: 0.82 to 0.89) and 0.85 (95% CI: 0.82 to 0.89), respectively (Figure 4). ROC curve analysis revealed a significantly greater diagnostic performance of hyperemic MBF than baseline MBF, MFR, and MFR_{corr} (all $p < 0.001$).

Diagnostic performance of the aforementioned perfusion parameters yielded similar results on a per-patient basis (Figure 4). Hyperemic MBF produced a significantly higher test performance than baseline MBF, MFR, and MFR_{corr} (all $p < 0.001$). No difference was seen in overall test performance between MFR and MFR_{cor} on both a per-vessel ($p = 0.88$) and per-patient ($p = 0.95$) level. The relationship between hyperemic MBF and estimated probability of CAD is shown in the Central Illustration. The optimal cutoff values for predicting hemodynamically significant CAD was 2.3 ml/min/g for hyperemic MBF and 2.5 ml/min/g for MFR. With these cutoff values, the diagnostic accuracy of hyperemic MBF was comparable on both a per-patient (86%) and per-vessel (85%) level (Figure 5), whereas the MFR demonstrated an accuracy of 78% and 81% on a per-patient and per-vessel basis (Figure 5, Table 3). Hyperemic MBF outperforms MFR as a perfusion parameter with regard to specificity ($p < 0.01$), and accuracy ($p < 0.01$).

When applying different FFR values of 0.65, 0.70, and 0.75 to indicate hemodynamic obstructive CAD, the optimal cutoff value for hyperemic MBF remained at 2.3 ml/min/g for all applied FFR thresholds (Figure 6). The diagnostic accuracy of hyperemic MBF in relation to different FFR cutoff values for defining hemodynamic obstructive CAD is shown in Table 4. Table 5 lists the diagnostic accuracy of quantitative [^{15}O]H_2O PET MPI for detecting angiographic obstructive CAD using ≥50% or ≥70% stenosis on ICA as thresholds. There was no difference in diagnostic performance of hyperemic MBF for detecting obstructive CAD, as indicated by FFR ≤0.80 between intracoronary and intravenous use of adenosine for measuring FFR.

In terms of FFR and myocardial perfusion, discordancy between hyperemic MBF, MFR, MFR_{corr}, and FFR was observed in 16%, 20%, and 21% of vessels, respectively (Figure 7). Regression analysis was performed to identify factors that affect myocardial perfusion (Table 6). According to univariate analysis, age ($p < 0.01$), female sex ($p < 0.001$), diabetes mellitus type 2 ($p = 0.01$), hypertension ($p = 0.02$), and FFR ≤0.80 ($p < 0.001$) all significantly affected hyperemic MBF. Multivariable analysis revealed that age, sex, hypertension, family history of CAD, and FFR were independently related to hyperemic MBF.

EFFECTS OF AGE AND SEX ON DIAGNOSTIC PERFORMANCE OF QUANTITATIVE [^{15}O]H_2O PET. The influence of sex and age on diagnostic accuracy

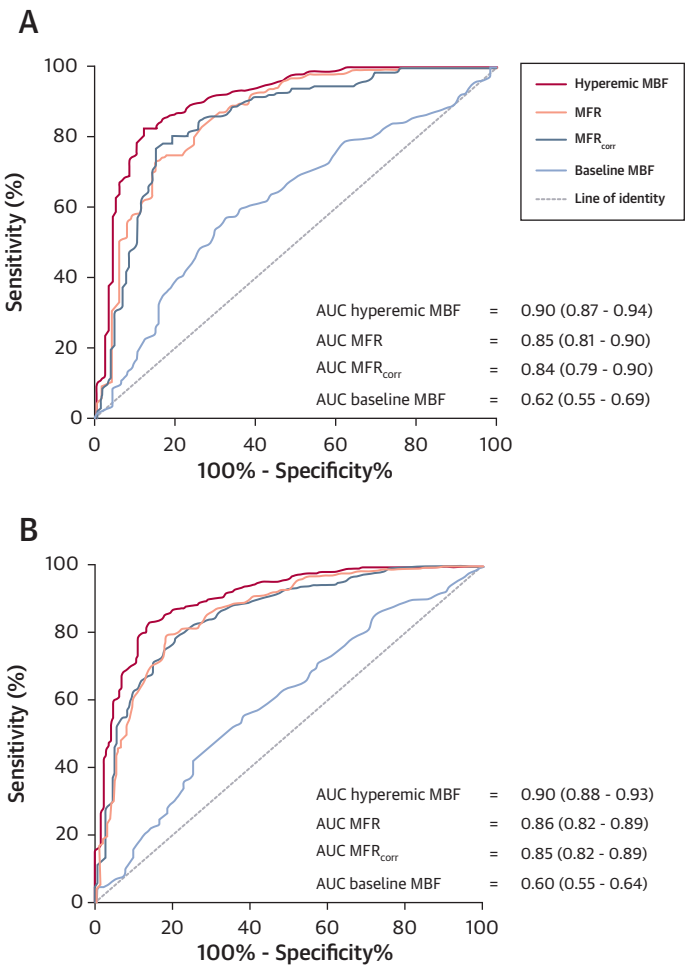

FIGURE 4 Diagnostic Performance of Quantitative PET Perfusion Parameters

Receiver-operator characteristic (ROC) curve analysis with corresponding area under the curves (AUCs) and 95% confidence intervals displaying the diagnostic performance of hyperemic MBF, MFR, MFR_{corr}, and baseline MBF for the detection of hemodynamically significant CAD as indicated by FFR on a **(A)** per-patient and **(B)** per-vessel level. Abbreviations as in Figures 1 to 3.

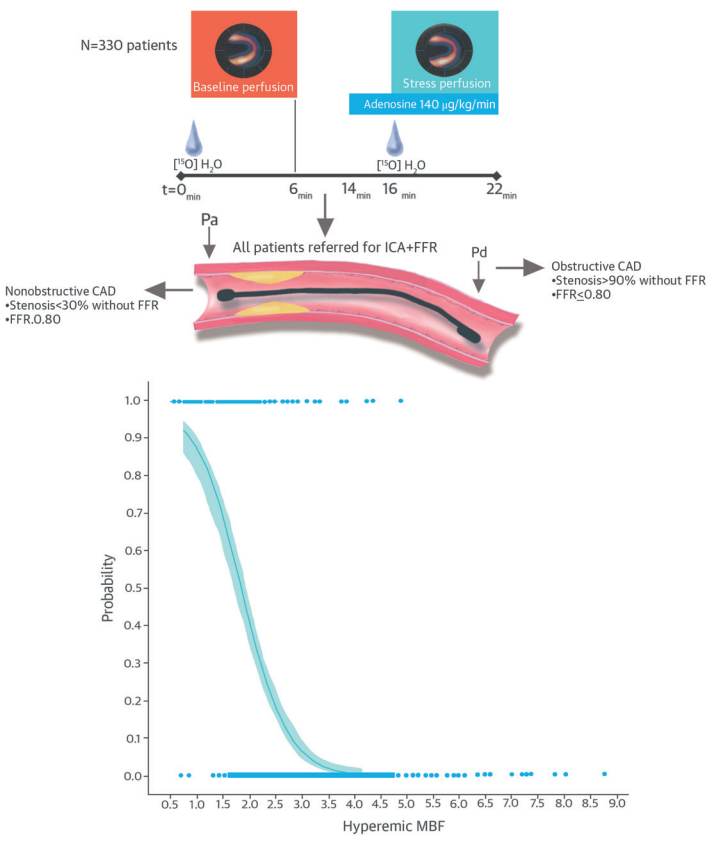

CENTRAL ILLUSTRATION Definition of Optimal Cut-Off Values for Absolute Cardiac Perfusion With High Accuracy Using Quantitative [^{15}O]H_2O PET

Probability of hemodynamically significant coronary artery disease (CAD) (y-axis) as defined by fractional flow reserve (FFR) versus quantitative positron emission tomography (PET) measurement of hyperemic myocardial blood flow (MBF) (x-axis). All patients underwent the shown [^{15}O]H_2O PET protocol and all patients were referred to the catheterization laboratory for invasive coronary angiography (ICA) in conjunction with FFR measurements. Optimal cutoff value for hyperemic MBF was 2.3 ml/min/g. Pa = pressure proximal to the lesion; Pd = pressure distal to the lesion.

of quantitative [^{15}O]H_2O PET was assessed (Table 7). Specificity, NPV, and diagnostic accuracy of quantitative [^{15}O]H_2O PET were significantly higher in female patients both on a per-patient and a per-vessel level. Age was categorized as ≤50 years, 51 to 60 years, 61 to 69 years, and ≥70 years. Although there was no significant difference in sensitivity across the various age groups, age significantly influenced specificity and diagnostic accuracy on a per-vessel level.

DISCUSSION

The main findings of this collaborative study are: 1) the optimal cutoff value of quantitative [^{15}O]H_2O PET MBF to detect hemodynamically significant CAD is 2.3 ml/min/g for hyperemic MBF and 2.5 for MFR; 2) MBF results indicate that diagnostic performance of absolute hyperemic MBF surpasses that of flow reserve; 3) quantitative [^{15}O]H_2O PET-derived MBF data provide an accuracy of 86% to detect flow-limiting CAD as defined according to abnormal FFR; and 4) age and sex are independent predictors of hyperemic MBF and both affect diagnostic performance of quantitative PET MBF.

One of the most fundamental issues when performing quantitative MPI is to define optimal thresholds of absolute perfusion. Previous studies reported discriminatory values of hyperemic MBF and MFR (10,12–15,17), but these trials were hampered by limitations inherent in single-center studies. Indeed, there is a lack of uniformity in reported cutoff values, which may also be due to the use of different PET radiotracers that likely provide different cutoff values because their kinetic properties are vastly different (3,4).

Hence, the increasing use of quantitative PET MPI in clinical practice necessitates generalizable and uniform cutoffs (2). The present study is, to the best of our knowledge, the first to determine cutoff values for MBF as assessed with [^{15}O]H_2O PET by using ICA together with FFR as the reference standard. In this analysis, the ideal cutoff for absolute stress perfusion was 2.3 ml/min/g and 2.5 for the perfusion reserve. The stress perfusion threshold of 2.3 ml/min/g is in line with the discriminatory value of <2.5 ml/min/g observed by Kajander et al. (15) but higher than that documented by Danad et al. (12) (1.86 ml/min/g), which may be attributed to methodological differences between the studies. Interestingly, Kajander et al. (12,15) incorporated, similar to the current study design, the routine use of FFR measurements to discern the functional relevance of CAD, which is considered the reference standard.

We also found a significantly higher area under the curve for hyperemic MBF compared with MFR to detect flow-limiting stenoses, which is also in line with previous studies (12,13,28). Dependency of MFR on both baseline and hyperemic MBF likely contributes to this finding because diminished stress perfusion does not necessarily cause a reduction in MFR. Although flow reserve has been shown to be of incremental value for prognosis (29), it seems that hyperemic MBF outperforms MFR in the noninvasive diagnosis of functionally relevant CAD. This finding paves the way for stress-only protocols, obviating the need of resting perfusion imaging with concomitant reduction in radiation dose and scan acquisition time.

DIAGNOSTIC PERFORMANCE OF QUANTITATIVE [^{15}O]H_2O PET MPI. Overall, the performance of [^{15}O]

H_2O PET-derived quantitative perfusion parameters shows promise for detecting obstructive CAD. Of all patients with functionally relevant stenosis, as indicated by FFR, only 13 (5%) were missed by quantitative hyperemic MBF imaging, resulting in a sensitivity of 89%; this finding mirrors previously published (single-center) studies showing a weighted sensitivity of 91% (4). However, most of these studies were conducted with static uptake images of ^{82}Rb and $^{13}NH_3$. More importantly, only 2 previous investigations used FFR as a reference standard for assessing hemodynamic relevance of intermediate lesions (12,15), whereas most studies relied on stenosis severity by ICA (4). The reliance on visual grading of coronary stenosis severity is potentially misleading and fails to accurately discern its physiological significance (30,31).

$[^{15}O]H_2O$ PET rules out obstructive CAD with a high NPV (92% per patient and 96% per vessel). Normal perfusion (>2.3 ml/min/g) excludes the presence of flow-limiting CAD. However, diminished stress perfusion does not necessarily imply presence of hemodynamically compromised epicardial disease. The observed PPV of 79% (59% on a per-vessel level) reflects the discrepancy between MBF and FFR. The proportion of discrepant findings between FFR and hyperemic MBF in the present study was ~16%, which is consistent with previous observations (32,33).

This mismatch between FFR and MBF does not necessarily represent the failure of either technique but likely indicates diffuse atherosclerotic or small vessel disease, which may not cause localized pressure gradients in FFR (33–36). The diagnosis of obstructive CAD is often based on the finding of a hemodynamically significant focal epicardial stenosis as indicated by FFR, reflecting hemodynamic relevance of epicardial atherosclerosis (24). PET MBF measures flow across the entire coronary artery network, consisting of both epicardial arteries and the microvasculature (17). Abnormal perfusion in the absence of significant epicardial pressure gradients is indicative of increased microvascular resistance (10,37,38), which may result from remodeling and vasoconstriction of arterioles due to endothelial dysfunction (10,37). Therefore, FFR and perfusion provide different information about the coronary artery tree and are not necessarily concordant (17,32,33). Consequently, it is impossible to distinguish between focal epicardial disease or small vessel or diffuse nonobstructive CAD based on absolute MBF or MFR alone. A hybrid imaging approach whereby PET is combined with anatomical imaging enables differentiation between microvascular and obstructive epicardial disease.

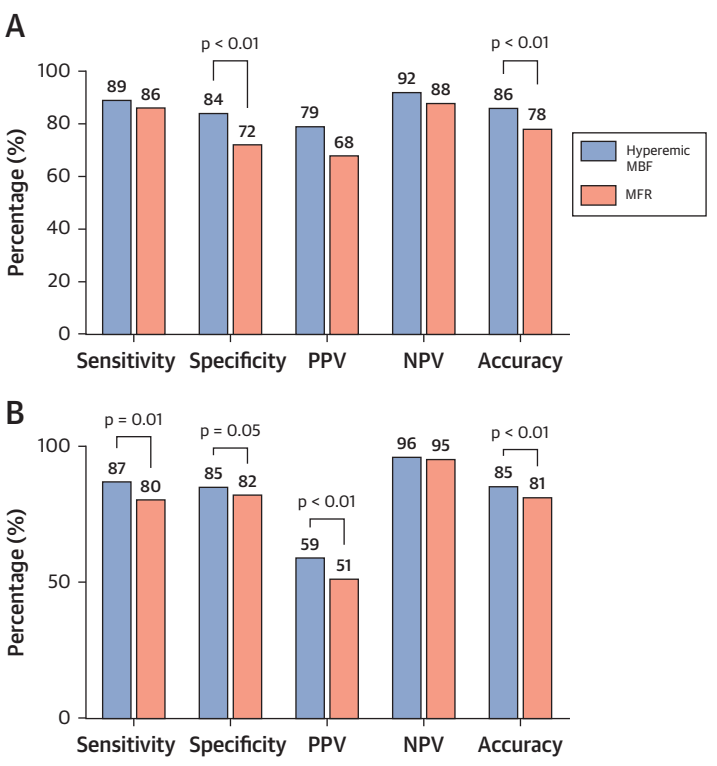

FIGURE 5 Diagnostic Performance of Hyperemic MBF and MFR PET Imaging

Sensitivity, specificity, positive predictive value (PPV), negative predictive value (NPV), and accuracy on a **(A)** per-patient and **(B)** per-vessel basis of quantitative PET MPI using hyperemic MBF and MFR, respectively, as a perfusion parameter. Abbreviations as in Figures 2 and 3.

EFFECTS OF AGE AND SEX ON THE DIAGNOSTIC ACCURACY OF QUANTITATIVE $[^{15}O]H_2O$ MBF. Impaired hyperemic MBF or MFR in the absence of obstructive CAD indicates microvascular dysfunction, which can be considered the functional counterpart of traditional CAD risk factors. These risk factors increase

TABLE 3 Results on a Per-Patient and Per-Vessel Level Using Hyperemic MBF as a Perfusion Parameter to Assess Diagnostic Accuracy of $[^{15}O]H_2O$ PET

	Epicardial Stenosis <30% or FFR >0.80	Epicardial Stenosis >90% or FFR ≤0.80
At a per-patient level		
Hyperemic MBF imaging	No (obstructive) CAD	Obstructive CAD
Positive (MBF ≤2.3 ml/min/g)	27	101
Negative (MBF >2.3 ml/min/g)	140	13
At a per-vessel level		
Hyperemic MBF imaging	No (obstructive) CAD	Obstructive CAD
Positive (MBF ≤2.3 ml/min/g)	106	151
Negative (MBF >2.3 ml/min/g)	583	23

FFR = fractional flow reserve; MBF = myocardial blood flow; PET = positron emission tomography; other abbreviations as in Table 1.

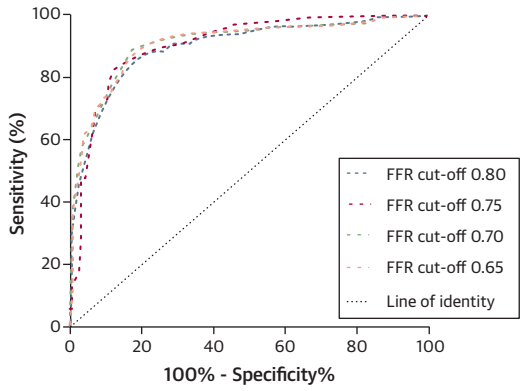

FIGURE 6 Diagnostic Performance of Quantitative PET According to Different FFR Thresholds

ROC curve analysis showing the diagnostic performance of hyperemic MBF on a per-vessel level using different FFR thresholds to indicate hemodynamically significant CAD. Abbreviations as in Figures 1 to 4.

coronary microvascular resistance and hence limit absolute myocardial perfusion (10,27,37), with sex and age both demonstrating an effect on hyperemic MBF (10,39,40); this may have important clinical implications. The present study found that both specificity and NPV are affected by age and sex but with no significant differences in accuracy across age. The prevalence of diffuse nonobstructive disease increases with age, which probably contributes to the observed discrepancy between absolute perfusion and FFR in elderly patients. Diffuse nonobstructive disease is shown to negatively impact MBF (33-36), whereas intracoronary pressures as reflected by FFR remain preserved.

TABLE 4 Diagnostic Accuracy of Quantitative [^{15}O]H_2O PET MPI Using Hyperemic MBF as a Perfusion Parameter

	FFR Cutoff: 0.65	FFR Cutoff: 0.70	FFR Cutoff: 0.75	FFR Cutoff: 0.80	p Value
Per-patient analysis					
Sensitivity	92	92	89	89	0.52
Specificity	78	80	81	84	0.62
NPV	95	95	93	92	0.26
PPV	67	71	74	79	0.22
Accuracy	83	84	84	86	0.66
Per-vessel analysis					
Sensitivity	94	93	90	87	0.20
Specificity	81	82	83	85	0.28
NPV	99	98	98	96	0.02
PPV	44	49	54	59	<0.01
Accuracy	83	84	85	85	0.70

Values are %.
MPI = myocardial perfusion imaging; NPV = negative predictive value; PPV = positive predictive value; other abbreviations as in Table 3.

TABLE 5 Diagnostic Accuracy of Quantitative [^{15}O]H_2O PET MPI for Detecting Angiographic Obstructive CAD

	Patient-Based Analysis	Vessel-Based Analysis
≥50% stenosis on ICA		
Sensitivity	85	80
Specificity	84	82
PPV	82	60
NPV	87	92
Accuracy	85	81
≥70% stenosis on ICA		
Sensitivity	94	89
Specificity	77	76
PPV	67	40
NPV	96	98
Accuracy	83	78

Values are %.
ICA = invasive coronary angiography; other abbreviations as in Tables 1, 3, and 4.

With regard to sex, diagnostic accuracy is significantly higher in women. This finding could partially be attributed to the lower prevalence of CAD in female patients. Although sex differences in hyperemic MBF have been reported (10,39), no separate quantitative MBF thresholds for men and women have been used to identify myocardial ischemia. Therefore, recognition of sex-related differences in quantitative PET will permit definition of optimal gender-specific thresholds when interpreting quantitative MBF results. It remains elusive whether the present findings are applicable only to quantitative MBF. Clearly, large prospective studies are warranted to determine whether age- and sex-corrected MBF reference values should be incorporated in diagnostic cardiac PET protocols.

STUDY LIMITATIONS. There are a number of limitations to our study. Although FFR was measured in numerous intermediate stenoses, some assumptions pertaining to missing values were made based on the findings of Tonino et al. (30), who reported that subtotal stenoses are virtually always (96%) hemodynamically significant. Also, only quantitative grading of PET images was performed and no comparison with visual MPI was provided, although previous studies have demonstrated that quantitative PET MPI outperforms visual PET diagnostically (8,9). Both intracoronary and intravenous administration of adenosine was used to achieve vasodilation during FFR measurements, although intravenous administration is generally the reference standard (31). However, there was no difference in diagnostic

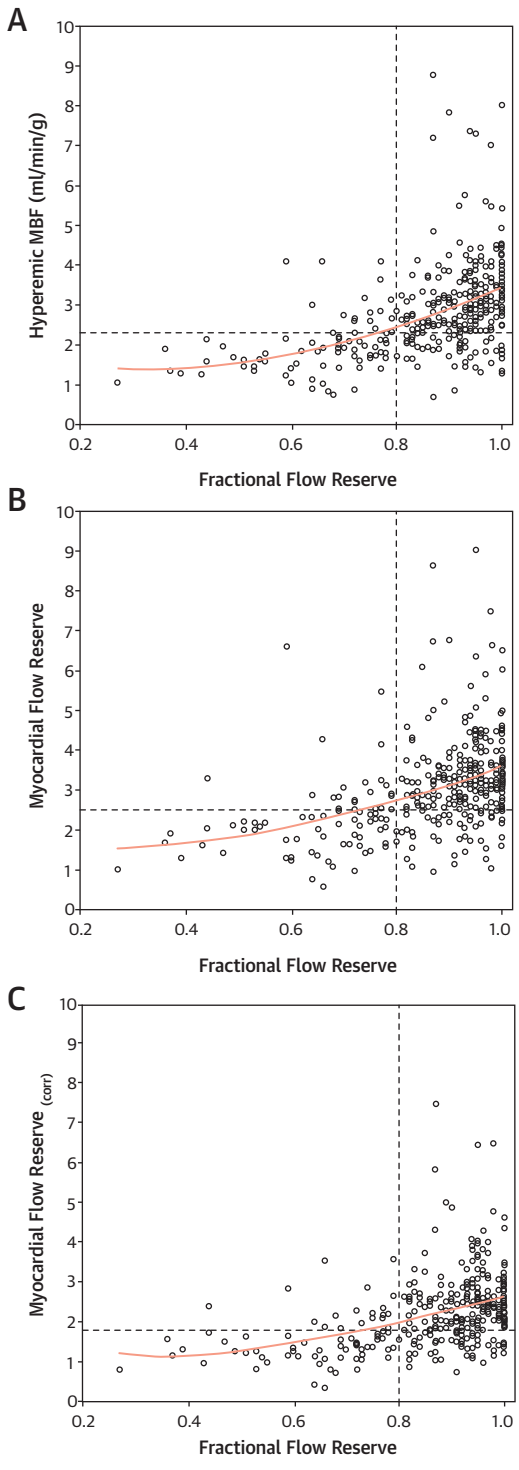

FIGURE 7 Quantitative Relationship Between Absolute Myocardial Perfusion and FFR

Scatterplots demonstrating the quantitative relationship between fractional flow reserve and **(A)** hyperemic MBF, **(B)** myocardial flow reserve, and **(C)** MFR_{corr}. Abbreviations as in Figures 1 and 3.

TABLE 6 Univariate and Multivariable Regression Analysis Describing the Relationship Between Hyperemic MBF, CAD Risk Factors, and Functional CAD Severity

	Univariate Analysis		Multivariable Analysis	
	β	p Value	β	p Value
Age, yrs	-0.02	<0.01	-0.02	0.02
(Female) sex	1.07	<0.001	0.89	<0.001
BMI, kg/m^2	-0.02	0.11	0.001	0.96
Diabetes mellitus type 2	-0.42	0.01	-0.27	0.13
Hypertension	-0.29	0.02	-0.24	0.04
Hypercholesterolemia	-0.007	0.95	0.10	0.35
Smoking history	-0.23	0.10	-0.21	0.08
Family history	-0.09	0.49	-0.24	0.04
FFR ≤0.80	-1.48	<0.001	-0.79	<0.001

Abbreviations as in Tables 1 and 3.

performance of quantitative PET to detect significant CAD as indicated by FFR achieved by either intracoronary or intravenous administration of adenosine.

Although care was taken to match coronary anatomy (obtained by using ICA) with PET perfusion territories, some misclassification between coronary arteries and their corresponding vascular regions in the PET scans may have occurred. In addition, vasoactive medication was not discontinued before

TABLE 7 The Influence of Sex and Age on the Diagnostic Performance of [^{15}O]H_2O Hyperemic MBF Imaging

	Sensitivity (%)	Specificity (%)	PPV (%)	NPV (%)	Accuracy (%)
Patient-based analysis					
Sex					
Male (n = 164)	90	70	80	85	82
Female (n = 117)	82	94	75	96	92
p value	0.27	<0.001	0.60	0.02	0.02
Age, yrs					
≤50 (n = 40)	92	79	65	96	83
51-60 (n = 96)	88	92	86	93	91
61-69 (n = 105)	87	85	81	89	86
≥70 (n = 40)	91	59	75	83	78
p value	0.93	<0.01	0.33	0.55	0.22
Vessel-based analysis					
Sex					
Male (n = 491)	84	75	59	92	78
Female (n = 372)	74	96	57	98	94
p value	0.19	<0.001	0.86	<0.001	<0.001
Age					
≤50 (n = 123)	78	87	50	96	85
51-60 (n = 297)	80	90	65	95	88
61-69 (n = 320)	82	84	58	95	83
≥70 (n = 123)	92	74	57	96	79
p value	0.54	<0.001	0.57	0.96	<0.001

Abbreviations as in Tables 3 and 4.

PET imaging, which may have negatively affected the sensitivity of quantitative PET. Furthermore, although the underlying modeling procedures were similar for all institutions, differences in defining arterial input function, spillover corrections, and automatic definition of myocardial segments between institutions may have influenced the generated perfusion values. Finally, obtained cutoff values may not be applicable to other PET flow tracers, such as $^{13}NH_3$ and ^{82}Rb, although several studies have shown that $^{13}NH_3$ provides comparable estimates of MBF over a wide range of flow values (41,42).

CONCLUSIONS

This is the first collaborative study to define cutoff values for absolute hyperemic MBF and MFR using ICA in conjunction with FFR as the reference standard. The optimal cutoff values for detecting flow-limiting stenosis were 2.3 ml/min/g for hyperemic MBF and 2.5 for MFR. Absolute hyperemic MBF measurements were superior to MFR for diagnosing hemodynamically significant CAD, implying that stress-only protocols would suffice in diagnostic PET protocols. $[^{15}O]H_2O$ PET provides high diagnostic accuracy, but both sex and age affect its accuracy.

REPRINT REQUESTS AND CORRESPONDENCE: Dr. Juhani Knuuti, Turku PET Centre, Turku University Hospital, P.O. Box 52, FI-20521 Turku, Finland. E-mail: juhani.knuuti@utu.fi.

PERSPECTIVES

COMPETENCY IN PATIENT CARE: Quantitative MPI may be used to help select patients for coronary angiography and reduce the need for invasive measurement of fractional flow reserve.

TRANSLATIONAL OUTLOOK: Comparative studies of contemporary single-photon emission computed tomography/CT and cardiac PET/computed tomography perfusion imaging technologies should be undertaken to determine their relative diagnostic utility.

REFERENCES

1. Bengel FM, Higuchi T, Javadi MS, Lautamaki R. Cardiac positron emission tomography. J Am Coll Cardiol 2009;54:1–15.

2. Saraste A, Kajander S, Han C, Nesterov SV, Knuuti J. PET: is myocardial flow quantification a clinical reality? J Nucl Cardiol 2012;19:1044–59.

3. Knuuti J, Kajander S, Maki M, Ukkonen H. Quantification of myocardial blood flow will reform the detection of CAD. J Nucl Cardiol 2009;16:497–506.

4. Danad I, Raijmakers PG, Knaapen P. Diagnosing coronary artery disease with hybrid PET/CT: it takes two to tango. J Nucl Cardiol 2013;20:874–90.

5. Lautamaki R, George RT, Kitagawa K, et al. Rubidium-82 PET-CT for quantitative assessment of myocardial blood flow: validation in a canine model of coronary artery stenosis. Eur J Nucl Med Mol Imaging 2009;36:576–86.

6. Araujo LI, Lammertsma AA, Rhodes CG, et al. Noninvasive quantification of regional myocardial blood flow in coronary artery disease with oxygen-15-labeled carbon dioxide inhalation and positron emission tomography. Circulation 1991;83:875–85.

7. Muzik O, Beanlands RS, Hutchins GD, Mangner TJ, Nguyen N, Schwaiger M. Validation of nitrogen-13-ammonia tracer kinetic model for quantification of myocardial blood flow using PET. J Nucl Med 1993;34:83–91.

8. Kajander SA, Joutsiniemi E, Saraste M, et al. Clinical value of absolute quantification of myocardial perfusion with (15)O-water in coronary artery disease. Circ Cardiovasc Imaging 2011;4:678–84.

9. Fiechter M, Ghadri JR, Gebhard C, et al. Diagnostic value of 13N-ammonia myocardial perfusion PET: added value of myocardial flow reserve. J Nucl Med 2012;53:1230–4.

10. Danad I, Raijmakers PG, Appelman YE, et al. Coronary risk factors and myocardial blood flow in patients evaluated for coronary artery disease: a quantitative [15O]H2O PET/CT study. Eur J Nucl Med Mol Imaging 2012;39:102–12.

11. Nesterov SV, Han C, Maki M, et al. Myocardial perfusion quantitation with 15O-labelled water PET: high reproducibility of the new cardiac analysis software (Carimas). Eur J Nucl Med Mol Imaging 2009;36:1594–602.

12. Danad I, Raijmakers PG, Appelman YE, et al. Hybrid imaging using quantitative H215O PET and CT-based coronary angiography for the detection of coronary artery disease. J Nucl Med 2013;54:55–63.

13. Hajjiri MM, Leavitt MB, Zheng H, Spooner AE, Fischman AJ, Gewirtz H. Comparison of positron emission tomography measurement of adenosine-stimulated absolute myocardial blood flow versus relative myocardial tracer content for physiological assessment of coronary artery stenosis severity and location. J Am Coll Cardiol Img 2009;2:751–8.

14. Muzik O, Duvernoy C, Beanlands RS, et al. Assessment of diagnostic performance of quantitative flow measurements in normal subjects and patients with angiographically documented coronary artery disease by means of nitrogen-13 ammonia and positron emission tomography. J Am Coll Cardiol 1998;31:534–40.

15. Kajander S, Joutsiniemi E, Saraste M, et al. Cardiac positron emission tomography/computed tomography imaging accurately detects anatomically and functionally significant coronary artery disease. Circulation 2010;122:603–13.

16. Chareonthaitawee P, Kaufmann PA, Rimoldi O, Camici PG. Heterogeneity of resting and hyperemic myocardial blood flow in healthy humans. Cardiovasc Res 2001;50:151–61.

17. Gould KL, Johnson NP, Bateman TM, et al. Anatomic versus physiologic assessment of coronary artery disease: guiding management decisions using positron-emission tomography (PET) as a physiologic tool. J Am Coll Cardiol 2013;62:1639–53.

18. Diamond GA, Forrester JS. Analysis of probability as an aid in the clinical diagnosis of coronary-artery disease. N Engl J Med 1979;300:1350–8.

19. Danad I, Raijmakers PG, Harms HJ, et al. Impact of anatomical and functional severity of coronary atherosclerotic plaques on the transmural perfusion gradient: a [15O]H2O PET study. Eur Heart J 2014.

20. Harms HJ, Knaapen P, de Haan S, Halbmeijer R, Lammertsma AA, Lubberink M. Automatic generation of absolute myocardial blood flow images using [15O]H2O and a clinical PET/CT scanner. Eur J Nucl Med Mol Imaging 2011;38:930–9.

21. Harms HJ, Nesterov SV, Han C, et al. Comparison of clinical non-commercial tools for automated quantification of myocardial blood flow using oxygen-15-labelled water PET/CT. Eur Heart J Cardiovasc Imaging 2014;15:431–41.

22. Czernin J, Muller P, Chan S, et al. Influence of age and hemodynamics on myocardial blood flow and flow reserve. Circulation 1993;88:62–9.

23. Austen WG, Edwards JE, Frye RL, et al. A reporting system on patients evaluated for coronary artery disease. Report of the Ad Hoc Committee for Grading of Coronary Artery Disease, Council on Cardiovascular Surgery, American Heart Association. Circulation 1975;51:5–40.

24. Pijls NH, De Bruyne B, Peels K, et al. Measurement of fractional flow reserve to assess the functional severity of coronary-artery stenoses. N Engl J Med 1996;334:1703–8.

25. Cerqueira MD, Weissman NJ, Dilsizian V, et al. Standardized myocardial segmentation and nomenclature for tomographic imaging of the heart. A statement for healthcare professionals from the Cardiac Imaging Committee of the Council on Clinical Cardiology of the American Heart Association. Int J Cardiovasc Imaging 2002;18:539–42.

26. DeLong ER, DeLong DM, Clarke-Pearson DL. Comparing the areas under two or more correlated receiver operating characteristic curves: a nonparametric approach. Biometrics 1988;44:837–45.

27. Kaufmann PA, Camici PG. Myocardial blood flow measurement by PET: technical aspects and clinical applications. J Nucl Med 2005;46:75–88.

28. Joutsiniemi E, Saraste A, Pietila M, et al. Absolute flow or myocardial flow reserve for the detection of significant coronary artery disease? Eur Heart J Cardiovasc Imaging 2014;15:659–65.

29. Herzog BA, Husmann L, Valenta I, et al. Long-term prognostic value of 13N-ammonia myocardial perfusion positron emission tomography added value of coronary flow reserve. J Am Coll Cardiol 2009;54:150–6.

30. Tonino PA, Fearon WF, De Bruyne B, et al. Angiographic versus functional severity of coronary artery stenoses in the FAME study fractional flow reserve versus angiography in multivessel evaluation. J Am Coll Cardiol 2010;55:2816–21.

31. Levine GN, Bates ER, Blankenship JC, et al. 2011 ACCF/AHA/SCAI guideline for percutaneous coronary intervention. J Am Coll Cardiol 2011;58:e44–122.

32. Meuwissen M, Chamuleau SA, Siebes M, et al. Role of variability in microvascular resistance on fractional flow reserve and coronary blood flow velocity reserve in intermediate coronary lesions. Circulation 2001;103:184–7.

33. Johnson NP, Kirkeeide RL, Gould KL. Is discordance of coronary flow reserve and fractional flow reserve due to methodology or clinically relevant coronary pathophysiology? J Am Coll Cardiol Img 2012;5:193–202.

34. Naya M, Murthy VL, Blankstein R, et al. Quantitative relationship between the extent and morphology of coronary atherosclerotic plaque and downstream myocardial perfusion. J Am Coll Cardiol 2011;58:1807–16.

35. Danad I, Raijmakers PG, Appelman YE, et al. Quantitative relationship between coronary artery calcium score and hyperemic myocardial blood flow as assessed by hybrid 15O-water PET/CT imaging in patients evaluated for coronary artery disease. J Nucl Cardiol 2012;19:256–64.

36. Liga R, Marini C, Coceani M, et al. Structural abnormalities of the coronary arterial wall—in addition to luminal narrowing—affect myocardial blood flow reserve. J Nucl Med 2011;52:1704–12.

37. Schindler TH, Schelbert HR, Quercioli A, Dilsizian V. Cardiac PET imaging for the detection and monitoring of coronary artery disease and microvascular health. J Am Coll Cardiol Img 2010;3:623–40.

38. Camici PG, Crea F. Coronary microvascular dysfunction. N Engl J Med 2007;356:830–40.

39. Duvernoy CS, Meyer C, Seifert-Klauss V, et al. Gender differences in myocardial blood flow dynamics: lipid profile and hemodynamic effects. J Am Coll Cardiol 1999;33:463–70.

40. Uren NG, Camici PG, Melin JA, et al. Effect of aging on myocardial perfusion reserve. J Nucl Med 1995;36:2032–6.

41. Bol A, Melin JA, Vanoverschelde JL, et al. Direct comparison of [13N]ammonia and [15O] water estimates of perfusion with quantification of regional myocardial blood flow by microspheres. Circulation 1993;87:512–25.

42. Nitzsche EU, Choi Y, Czernin J, Hoh CK, Huang SC, Schelbert HR. Noninvasive quantification of myocardial blood flow in humans. A direct comparison of the [13N]ammonia and the [15O]water techniques. Circulation 1996;93:2000–6.

KEY WORDS myocardial blood flow, myocardial flow reserve, receiver-operator characteristic curve, sensitivity, specificity